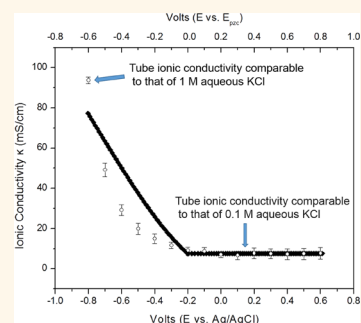


# Voltage Charging Enhances Ionic Conductivity in Gold Nanotube Membranes

Peng Gao and Charles R. Martin\*

Department of Chemistry, University of Florida, Gainesville, Florida 32611, United States

**ABSTRACT** Ionically conductive membranes are used in many electrochemical processes and devices, including batteries, fuel cells, and electrolyzers. In all such applications, it is advantageous to use membranes with high ionic conductivity because membrane resistance causes a voltage loss suffered by the cell. We describe here a method for enhancing ionic conductivity in membranes containing small diameter (4 nm) gold nanotubes. This entails making the gold nanotube membrane the working electrode in an electrochemical cell and applying a voltage to the membrane. We show here that voltage charging in this way can increase membrane ionic conductivity by over an order of magnitude. When expressed in terms of the ionic conductivity of the electrolyte,  $\kappa$ , within an individual voltage-charged tube, the most negative applied voltage yielded a  $\kappa$  comparable to that of 1 M aqueous KCl, over 2 orders of magnitude higher than  $\kappa$  of the 0.01 M KCl solution contacting the membrane.



**KEYWORDS:** electrolyte resistance · electrochemical energy · membrane resistance · voltage charging · ionic conductivity · gold nanotubes · nanotube membranes · electrochemistry

Ionically conductive membranes are used in many electrochemical processes and devices, including batteries, fuel cells, and electrolyzers.<sup>1–6</sup> These membranes act as separators to prevent ohmic contact between the anode and the cathode and often are needed to prevent mixing of the cathode and anode solutions. Such membranes must be ionically conductive to allow ionic current to flow through the cell. Regardless of the application, it is advantageous to use membranes with high ionic conductivity because membrane resistance causes a voltage loss suffered by the cell.<sup>4,5</sup> This voltage loss means that more energy is needed to drive an industrial electrolytic process and less energy is obtained from a battery or fuel cell.

We have been investigating conductivity in membranes containing gold nanotubes<sup>7–13</sup> prepared by the template-synthesis method.<sup>14,15</sup> These tubes have monodisperse inside diameters and run through the entire thickness of the membrane. Ionic conductivity can be enhanced in these membranes by attaching ionizable groups to the tube walls.<sup>7</sup> In the presence of a suitable solvent (typically an aqueous solution), these ionizable groups dissociate, yielding fixed

charge carriers on the tube wall and mobile counterions in the tube solution. These mobile counterions carry charge through the membrane.

An alternative approach for incorporating fixed charge on the tube walls and mobile counterions in the tube solution entails making the gold nanotube membrane the working electrode in an electrochemical cell and applying a voltage to the nanotubes.<sup>8–12</sup> At negative applied voltages, this causes excess electrons to be injected along the tube walls.<sup>9</sup> This requires charge-balancing cations to be incorporated into the solution filling the tubes. We call these excess cations because they were not present in the tube solution before the membrane was voltage charged. This concept is illustrated in Figure 1A, which shows the front of a single negatively charged tube along with some of the electrolyte solution in front of the tube. The key conceptual point is the high concentration of cations within the tube relative to the surrounding solution. These are the excess cations brought in by voltage charging.

If the tube diameter is sufficiently small, these excess ions could dominate ionic conductivity in the tube, and this might

\* Address correspondence to crmartin@chem.ufl.edu.

Received for review May 15, 2014 and accepted July 25, 2014.

Published online July 25, 2014  
10.1021/nn502642m

© 2014 American Chemical Society

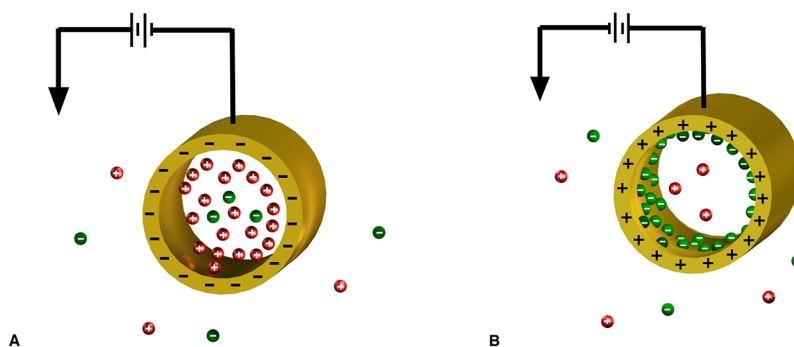


**Figure 1.** (A) Schematic illustration of a negatively charged gold nanotube with incorporated charge-balancing cations (labeled +). The negative charge was obtained by applying a negative voltage to the gold nanotube membrane. The nanotube membrane is immersed in an electrolyte solution (see text). (B) Schematic of positively charged gold nanotube with incorporated charge-balancing chloride anions (labeled -). As illustrated conceptually, these anions adsorb to the gold tube wall and are immobile.

provide a route for increasing membrane conductivity. Indeed, membrane conductivity would, in principle, be voltage-dependent with the highest conductivities achieved at the highest values of either negative or positive applied voltage. This phenomenon has recently been demonstrated,<sup>16</sup> but those studies involved a porous gold electrode in contact with pure water; that is, no electrolyte was added. The question of how applied voltage affects membrane conductivity for a membrane immersed into a real electrolyte solution has yet to be investigated.

We show here that voltage-charging gold nanotube membranes in aqueous KCl solution can increase membrane conductivity but, in contrast to the pure water case,<sup>16</sup> only at negative applied voltages. We present a model based on anion adsorption that explains this observation. At the highest negative voltage, the membrane conductivity increased by over an order of magnitude. When expressed in terms of the ionic conductivity of the electrolyte,  $\kappa$ , within a tube, the most negative applied voltage yielded a  $\kappa$  comparable to that of 1 M aqueous KCl, over 2 orders of magnitude higher than  $\kappa$  of the 0.01 M KCl solution contacting the membrane.

## RESULTS AND DISCUSSION

**Electrochemical Cell.** A U-tube-based electrochemical cell was used,<sup>8–12</sup> in which the membrane separated two identical electrolyte solutions (Figure 2). The electrolyte solution used throughout these studies was 0.01 M KCl. The bipotentiostat (B) allowed us to apply a voltage to the membrane and, at the same time, apply a voltage difference across the membrane. The transmembrane voltage was used to measure the ionic conductivity of the electrolyte-filled tubes,  $\kappa$  (see Experimental Section for details).

**Membrane Cyclic Voltammetry.** The voltage-charging concept being investigated here involves storage of excess electronic charge on the nanotube walls at the wall/tube–solution interface. This will only occur over a voltage window where there are no

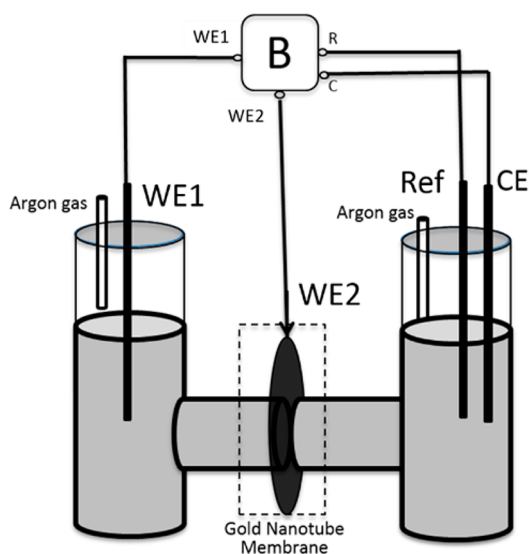


**Figure 2.** Electrochemical cell. A bipotentiostat (B) was used to independently control the voltage applied to the membrane with working electrode 2 (WE2) and the voltage applied across the membrane, WE1. A Ag/AgCl reference electrode (BASi, MF-2079) was used as WE1 and as the electrode labeled ref. A Pt wire was used as the counter electrode (CE). ref and CE were shared by both of the channels of the bipotentiostat.

Faradaic reactions; in electrochemical parlance, the gold nanotube membrane must act like an ideally polarized electrode.<sup>17</sup> Cyclic voltammetry was used to determine the potential window where the membrane acts in this way. Since no transmembrane voltage was needed for these experiments, the bipotentiostat (B, Figure 2) was used as a single potentiostat.

Cyclic voltammograms over a voltage window from  $-1.2$  to  $+1.2$  V (vs Ag/AgCl) were obtained (Supporting Information Figure S1). Reduction of the solvent water was observed at voltages negative of about  $-0.8$  V, and water oxidation was seen at voltages positive of about  $+0.6$  V. To avoid these Faradaic reactions, a voltage window of  $-0.8$  to  $+0.6$  V (vs Ag/AgCl) was used for our studies. Currents obtained over this voltage window are by-in-large non-Faradaic (Figure 3).

Using this restricted voltage window has an added advantage. Because our membranes are composed of an electronically conductive material, the membrane will be polarized when a voltage is applied across the membrane, as is done in our measurement of  $\kappa$ . At sufficiently high transmembrane voltages, the membrane might act as a bipolar electrode<sup>18</sup> with water oxidation occurring at one face and water reduction at the other. The  $-0.8$  to  $+0.6$  V (vs Ag/AgCl) voltage range avoids this potentially complicating issue.

**Effect of Voltage Charging on Nanotube Ionic Conductivity,  $\kappa$ .**  $\kappa$  was obtained from current–voltage ( $I$ – $V$ ) curves associated with ion transport through the tubes (Figure 4). The slope of the  $I$ – $V$  curve is the ionic conductance of the membrane ( $G_m$ ,  $\text{ohm}^{-1}$ ).  $\kappa$  is related to  $G_m$  via<sup>19</sup>

$$\kappa = lG_m/n\pi r_p^2 \quad (1)$$

where  $l$  is the membrane thickness, and  $n$  is the number of tubes in the membrane sample (see Experimental Section for details).

$I$ – $V$  curves for a membrane containing tubes having an inside radius,  $r_p$ , of 8 nm, do not change

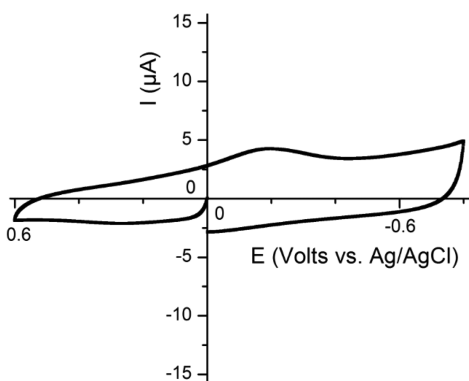


Figure 3. Cyclic voltammogram for a gold nanotube membrane with tube radius  $r_p = 2$  nm in degassed 0.01 M KCl. Scan rate =  $100 \text{ mV s}^{-1}$ .

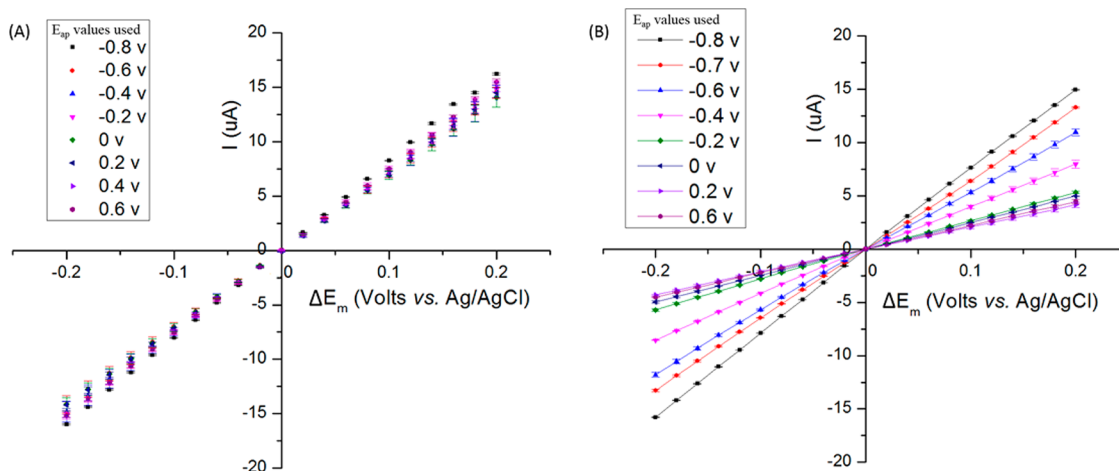
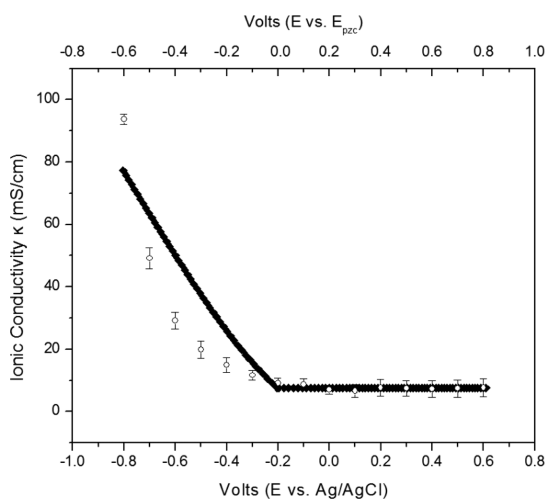


Figure 4. Current–voltage curves associated with ion transport through gold nanotube membranes as a function of voltage applied to the membrane,  $E_{ap}$ . The legend shows the  $E_{ap}$  values used. The electrolyte was degassed 0.01 M KCl. Inside tube radius,  $r_p$ , was (A) 8 nm and (B) 2 nm.

with voltage applied to the membrane,  $E_{ap}$  (Figure 4A). Within experimental error,  $\kappa$  values obtained from the slopes of these curves (eq 1) are identical. This is because an enhancement in conductivity is only observed when the thickness of the electrical double layer (where the excess ions are located<sup>20</sup>) is comparable to the tube radius. If this is not the case, conductivity is dominated by the ions partitioned into the tubes from the contacting electrolyte solution. Because the double layer is roughly 3 nm thick for 0.01 M KCl,<sup>20</sup> this criterion is not satisfied for the  $r_p = 8$  nm membrane (Figure 4A).

In contrast, when analogous voltage-charging experiments are done with membranes having  $r_p = 2$  nm tubes, the slopes of the  $I$ – $V$  curves change significantly with  $E_{ap}$  (Figure 4B). That the slopes change with  $E_{ap}$  demonstrates that voltage charging does change tube conductivity for these smaller radius tubes. The  $\kappa$  values obtained are plotted against  $E_{ap}$  in Figure 5. Note that Figure 5 has two voltage axes,  $E_{ap}$  vs Ag/AgCl at the bottom and  $E_{ap}$  versus  $E_{pzc}$  at the top.  $E_{pzc}$  is the potential of zero charge, where there is no excess charge on the electrode surface.<sup>21</sup> As per a prior study of gold electrodes immersed into 0.01 M KCl solution, we use  $E_{pzc} = -0.2$  V vs Ag/AgCl.<sup>22</sup> Because for the voltage-charged membrane concept  $E_{ap}$  versus  $E_{pzc}$  is the more relevant voltage axis,  $E_{ap}$  values discussed henceforth will be versus  $E_{pzc}$ .

Figure 5 shows that tube conductivity is highest at the largest value of negative  $E_{ap}$  ( $-0.6$  V). The  $\kappa$  value obtained ( $94 \text{ mS cm}^{-1}$ ) is comparable to that of 1 M KCl and is over an order of magnitude higher than  $\kappa$  at  $E_{pzc}$  (Figure 5). As discussed qualitatively earlier, this high conductivity results because the excess negative charge on the tube walls at  $E_{ap} = -0.6$  V causes charge-balancing  $\text{K}^+$  to enter the tubes (Figure 1A). Since conductivity is proportional to the concentration of charge carriers,  $-0.6$  V gives the highest conductivity.



**Figure 5.** Plots of ionic conductivity of the tube solution,  $\kappa$ , versus applied voltage for the  $r_p = 2$  nm membrane. The open circles are the experimental data; error bars are associated with data obtained from three identically prepared membranes. The solid curve is a simulation based on our revised (anion-adsorption-based) GCS model (see text). The lower voltage axis is vs the Ag/AgCl reference. The upper voltage axis is versus the potential of zero charge.<sup>22</sup>

The similarity between this tube conductivity and 1 M KCl indicates, qualitatively, that at  $E_{ap} = -0.6$  V, the ionic strength within the tubes is comparable to that of 1 M KCl. This conductivity is 2 orders of magnitude higher than the conductivity of the 0.01 M KCl solution on either side of the membrane. These data prove the main objective of this effort—that voltage charging can be used to enhance membrane conductivity, relative to the uncharged membrane.

Figure 5 also shows that tube conductivity decreases as  $E_{ap}$  is moved positive of the  $-0.6$  V limit. This was the anticipated result because, until  $E_{ap} = E_{pzc}$ , the quantity of excess electrons injected along the tube wall decreases as  $E_{ap}$  is moved positively. If the simplest model<sup>16</sup> is correct, tube conductivity should then increase at  $E_{ap}$  positive of  $E_{pzc}$  as excess positive charge is injected along the tube walls. This is because, in analogy to the excess  $K^+$  incorporated at negative  $E_{ap}$  (Figure 1A), charge-balancing  $Cl^-$  must be incorporated into the tubes at positive  $E_{ap}$ , causing an increase in tube ionic strength and a corresponding increase in tube conductivity. Put another way, the simplest theory<sup>16</sup> predicts that the  $\kappa$  versus  $E_{ap}$  curve should be symmetrical about  $E_{pzc}$  with conductivity increasing at both negative and positive value of  $E_{ap}$ .

Such symmetrical  $\kappa$  versus  $E_{ap}$  plots were observed experimentally, and modeled theoretically, in an experiment with a porous gold electrode in contact with pure water.<sup>16</sup> In contrast, when the gold nanotube membrane is in contact with 0.01 M KCl, the  $\kappa$  versus  $E_{ap}$  plot is not symmetrical because  $\kappa$  does not increase with  $E_{ap}$  at values positive of  $E_{pzc}$  (Figure 5). We propose that an anion-adsorption model can explain this observation.

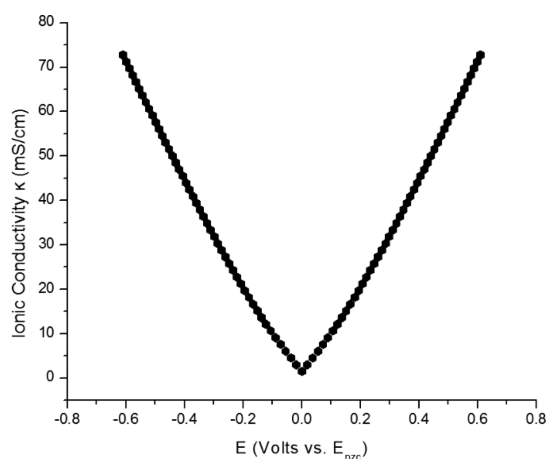


**Figure 6.** Simulated tube ionic conductivity data obtained from the simple GCS model<sup>16</sup> for the  $r_p = 2$  nm membrane in contact with 0.01 M KCl.

**Theoretical Model with Specific Anion Adsorption.** A Gouy–Chapman–Stern (GCS) model<sup>16</sup> can be used to calculate the quantity of excess charge present on the tube wall ( $Q$ ,  $\mu C\text{ cm}^{-2}$ ) at any value of  $E_{ap}$  (eq 2)

$$Q = 372C_0^{1/2} \sinh \left[ 19.46 \left( E_{ap} - \frac{Q}{C_{Au}} \right) \right] \quad (2)$$

where  $C_0$  is the concentration of bulk electrolyte solution in contact with the membrane (in  $\text{mol cm}^{-3}$ ), and  $C_{Au}$  is the capacitance of the gold/electrolyte interface along the tube wall ( $\mu F\text{ cm}^{-2}$ ). The ionic conductivity of the tube solution,  $\kappa$ , is related to  $Q$  via eq 3.

$$\kappa = C_0 \times F \times (\mu_K + \mu_{Cl}) + 2 \times \mu_i \times Q/r_p \quad (3)$$

The first term in eq 3 accounts for electrolyte partitioned into the tube from the contacting solution phase; we assume that this concentration is identical to that in the contacting solution. Since equivalent numbers of cations and anions are incorporated from the contacting solution, the mobilities of both  $K^+$  ( $\mu_K$ ) and  $Cl^-$  ( $\mu_{Cl}$ ) are included. It is assumed that these mobilities are identical to the values for these ions in bulk solution.<sup>23</sup> The second term in eq 3 accounts for the excess ions incorporated into the tube because of voltage charging. The parameter  $\mu_i$  is the bulk-solution mobility for the incorporated excess ion, either  $K^+$  for voltages negative of  $E_{pzc}$  or  $Cl^-$  for positive  $E_{ap}$ .

Figure 6 shows a simulation, based on the simple GCS model, of tube ionic conductivity versus  $E_{ap}$ . As per our experimental data, it was assumed that the membrane contained tubes with  $r_p = 2$  nm and that the contacting electrolyte solution was 0.01 M KCl. As expected, the simulated tube ionic conductivity increases symmetrically about  $E_{pzc}$  for both positive and negative values of  $E_{ap}$ . A similar curve was observed experimentally for a porous gold electrode immersed in pure water, but the valley in  $\kappa$  around  $E_{pzc}$  was much wider along the voltage axis.<sup>16</sup> This is

because the ionic strength of pure water is  $10^{-7}$  M, and less charge is stored at any  $E_{ap}$  when the ionic strength of the contacting solution phase is low (eq 2).

The simulated curve in Figure 6 shows two major disagreements with our experimental data (Figure 5). First, the  $\kappa$  value at  $E_{pzc}$  obtained experimentally is about 4 times higher than the value obtained from the simulation. Again, the simulation assumes that the ionic strength within the tubes at  $E_{pzc}$  is the same as that of the bulk solution value. The experimental data show that the tube ionic strength is, in fact, higher. This indicates that there is charge on the tube wall at  $E_{pzc}$  and the simple GCS model does not account for this charge.

It is well-known that  $\text{Cl}^-$  adsorbs to gold surfaces,<sup>24–26</sup> and we propose that the charge on the tube walls at  $E_{pzc}$  is due to this adsorbed  $\text{Cl}^-$ .  $\text{Cl}^-$  adsorption causes the tube ionic strength to be higher than that of the bulk electrolyte because, to a first approximation, each adsorbed  $\text{Cl}^-$  causes a charge-balancing  $\text{K}^+$  to enter the tube. This indicates that eq 3 must be modified to account for the quantity of adsorbed  $\text{Cl}^-$ ,  $Q_{Ad}$  (eq 4).

$$\kappa = C_0 \times F \times (\mu_K + \mu_{Cl}) + 2 \times \mu_i \times Q_{Ad}/r_p + 2 \times \mu_i \times Q/r_p \quad (4)$$

Equation 4 assumes that the quantity of charge-balancing  $\text{K}^+$  incorporated into the tube is identical to  $Q_{Ad}$  and that the mobility of these ions is identical to that for  $\text{K}^+$  in bulk solution.

Our experimental data (Figure 5) gave a value of  $Q_{Ad} = 0.79 \mu\text{C cm}^{-2}$ , and in our revised GCS-based model (solid curve in Figure 5), we use this value to raise the simulated  $\kappa$  at  $E_{ap} = E_{pzc}$  to the experimental curve. We also assume that  $Q_{Ad}$  is independent of  $E_{ap}$  (*vide infra*). It is worth noting that the experimental value of  $Q_{Ad}$  for the  $r_p = 2$  nm tubes is significantly smaller than values obtained for (flat) gold electrodes immersed into KCl solutions.<sup>24,25,27</sup> This suggests that anion adsorption might be suppressed in such very small radius gold tubes.

The second discrepancy between the simple GCS simulation (Figure 6) and our experimental data (Figure 5) is that tube conductivity does not increase with  $E_{ap}$  at values positive of  $E_{pzc}$ . We propose that this can, again, be explained by  $\text{Cl}^-$  adsorption. At positive  $E_{ap}$  values, positive charge is injected along the tube walls, resulting in the incorporation of charge-balancing chloride anions. However, in contrast to the excess  $\text{K}^+$  incorporated at negative values of  $E_{ap}$  (Figure 1A), adsorption causes the excess  $\text{Cl}^-$  incorporated to be immobile (Au–Cl bond strength 280 kJ/mol<sup>28</sup>).

As illustrated conceptually in Figure 1B, because the incorporated  $\text{Cl}^-$  is immobile, there is no enhancement in tube ionic strength as is observed at negative applied voltages (Figure 1A). As a result, in agreement with our data (Figure 5), conductivity is not enhanced at positive applied voltages. Put another way, while a

highly cation-conductive state could be achieved, an analogous highly anion-conductive state could not. To simulate this effect, we set the mobility for the  $\text{Cl}^-$  incorporated due to voltage charging at positive  $E_{ap}$  (second term in eq 4) to zero. In agreement with the experimental data, this causes  $\kappa$  to be independent of  $E_{ap}$  at positive values (solid curve Figure 5).

Our prior studies, where potentiometric experiments were used to show that voltage charging could convert a gold nanotube membrane from a cation-conductive to an anion-conductive state, support this model.<sup>9</sup> When those experiments were done using an ion that does not adsorb to gold,  $\text{F}^-$ , the membrane could successfully be voltage-switched between nearly ideal cation- and anion-conductive states. However, when an adsorbing anion was used,  $\text{Br}^-$ , just as in our case (Figure 5), the anion-conductive state could not be obtained.<sup>9</sup> This inability to obtain the anion-conductive state is another way to think about the flat  $\kappa$  versus  $E_{ap}$  response seen at voltages positive of  $E_{pzc}$  in Figure 5.

While this modified, adsorption-based, GCS model reproduces the general shape of the experimental  $\kappa$  versus  $E_{ap}$  curve (Figure 5), quantitative differences persist. This can be seen at negative values of  $E_{ap}$  where the experimental data are, in general, less than the values predicted by the simulation. We believe that this disagreement results from our assumption (*vide supra*) that the quantity of adsorbed  $\text{Cl}^-$  is independent of  $E_{ap}$ . Kolics *et al.* found that the quantity of  $\text{Cl}^-$  adsorbed to gold electrodes is highest at applied voltages well positive of  $E_{pzc}$  and decreases as  $E_{ap}$  is made more negative.<sup>24</sup> This suggests that the  $Q_{Ad}$  term in eq 4 should, in fact, decrease with applied voltage at negative  $E_{ap}$  values. In closer agreement with the experimental data, this would cause the simulated values of  $\kappa$  to be smaller than the values in our current simulation, which assumes constant  $Q_{Ad}$ .

However, the experimental  $\kappa$  at the most negative  $E_{ap}$  is greater than the simulated value, and this cannot be accounted for by the proposed voltage dependence of  $Q_{Ad}$ . Returning to the cyclic voltammogram in Figure 3, we see a small rise in the background currents at the most negative values of  $E_{ap}$ . This indicates that some Faradaic redox reaction is being activated at such high negative  $E_{ap}$ . If this reaction is water reduction, hydroxide ions would be liberated into the tubes, and this might account for the high value of  $\kappa$  observed at  $E_{ap} = -0.6$  V. Other issues that might cause discrepancies between the experimental and simulated data include the limitations of the GCS model itself,<sup>20</sup> our assumption that the mobilities of the incorporated excess ions are identical to their bulk-solution values and independent of the voltage applied to the membrane, and the electronic polarization of the membrane in the electric field used to measure the membrane conductivity.



## CONCLUSIONS

We have shown that voltage charging can be used to increase membrane conductivity for membranes containing small-radius ( $r_p = 2$  nm) gold nanotubes. At the most negative applied voltage, conductivity increased by over an order of magnitude relative to the conductivity at the potential of zero charge. However, such increases in conductivity are only seen at applied voltages negative of  $E_{pzc}$ . Conductivity does not change with applied voltage at values positive of  $E_{pzc}$ . We have developed an anion ( $Cl^-$ )-adsorption-based model that accounts for this observation.

Since many anions adsorb to gold from aqueous solution,<sup>29</sup> a lack of conductivity change at positive  $E_{ap}$  might be the general result. However, in our prior work, we showed that adsorption of a small neutral thiol could prevent anion adsorption, allowing for successful voltage charging between cation- and anion-conductive states in the presence of an adsorbing anion.<sup>9</sup> This concept of preventing anion adsorption by applying a neutral blocking species might provide a route for achieving both highly anion- and

cation-conductive states (Figure 6) even when an adsorbing anion is present. It is also worth noting that anion adsorption may not be a problem in non-aqueous solvents such as those used in Li-ion batteries.<sup>30</sup> This is because the anions used (e.g.,  $PF_6^-$ ) have lower charge densities and are more weakly coordinating.

Finally, if the goal is to use this approach to make highly conductive membranes for electrochemical devices, it is important to point out that the template membrane used to prepare these gold nanotubes is only about 0.4% porous.<sup>31</sup> If practical voltage-charged membranes are to be developed, a template with much higher porosity would be required. For example, the Celgard membranes used in Li-ion batteries have porosities on the order of 40%.<sup>5</sup> Porous alumina membranes can have porosities as high as 50%,<sup>32</sup> and we have shown that gold<sup>32</sup> and carbon<sup>33–35</sup> nanotubes can be deposited into such membranes. This suggests that porous alumina templates might be a good starting point for preparing the next generation of voltage-charged membranes.

## EXPERIMENTAL SECTION

**Materials.** Polycarbonate membrane filters (Poretics Corporation, 6  $\mu m$  thick, 30 nm diameter pores, and  $6 \times 10^8$  pores  $cm^{-2}$ ) were used as the template to prepare the gold nanotubes. Anhydrous  $SnCl_2$  (Aldrich),  $AgNO_3$  (Spectrum), trifluoroacetic acid,  $Na_2SO_3$ , ammonium hydroxide, formaldehyde, anhydrous methanol, 1-propanethiol (Aldrich), concentrated  $HNO_3$  (Mallinckrodt), and sulfuric acid were used as received. Commercial gold-plating solution (Oromorse Part B) was obtained from Technic, Inc. Purified water was obtained by passing house-distilled water through a Barnstead E-Pure water purification system.

**Membrane Preparation.** The electroless plating method used to make the gold nanotube membrane has been described previously.<sup>9,31</sup> This method causes gold to deposit both along the pore wall and on the membrane faces. As a result, the membrane gets embedded within a collection of open-ended gold nanotubes that run from one face of the membrane to the other. These nanotubes are connected at both membrane faces by thin gold surface films.<sup>8</sup> The effective inner tube radius,  $r_p$ , of the gold nanotubes can be controlled by varying the electroless plating time.<sup>9,14,31</sup> Nanotubes with  $r_p = 8$  nm and  $r_p = 2$  nm were prepared for these studies.

**Electrochemical Cell.** The cell used (Figure 2) and the membrane-mounting procedure have been described previously.<sup>9,36</sup> Briefly, the membrane is mounted between the two halves of a U-tube cell, and each half-cell is filled with 0.01 M KCl. Ohmic contact was made to the membrane by attaching a strip of conductive copper tape (3M, #1181) to the gold surface film covering one face of the membrane.<sup>8</sup> In addition to applying a voltage to the membrane, membrane conductivity was measured by applying a potential difference across the membrane. As a result, a bipotentiostat (CH 700E, B in Figure 1) was used.

**Measurement of Inside Tube Radius,  $r_p$ .** An electrochemical method was used to determine  $r_p$ .<sup>37,38</sup> Working electrode 2 (WE2, Figure 2) was not used in this experiment, and the bipotentiostat worked as a single potentiostat. Working electrode (WE1) was used to apply a potential difference across the membrane ( $\Delta E_m$ ) relative to the reference electrode (ref) on the other side (Figure 2).  $\Delta E_m$  drives ions through the nanotubes,

yielding an ionic current, which is measured. The current was measured at various values of  $\Delta E_m$ . The resulting current–voltage ( $I$ – $V$ ) curves were used to calculate the membrane resistance, which was used to calculate  $r_p$ .<sup>37,38</sup>

**Membrane Cyclic Voltammetry.** The bipotentiostat was used as a single potentiostat for these studies. Voltammograms were obtained by scanning the potential applied to the membrane relative to the reference electrode.<sup>31</sup> The electrolyte on both sides of the membrane (0.01 M KCl) was degassed by bubbling Ar gas for 20 min and kept degassed by passing Ar over the solutions during the measurements.

**Measurement of  $\kappa$ .** Both channels of the bipotentiostat were used for these experiments. As per the measurement of  $r_p$ , WE1 was used to obtain an  $I$ – $V$  curve associated with ion transport through the tubes in the membrane. Such  $I$ – $V$  curves were obtained at various values of potential applied, *via* WE2, to the membrane (Figure 2). The slope of the  $I$ – $V$  curve is the ionic conductance ( $G_m$ ,  $ohm^{-1}$ ), which is related to  $\kappa$  *via* eq 1.

**Conflict of Interest:** The authors declare no competing financial interest.

**Acknowledgment.** The work was supported by the Nanostructures for Electrical Energy Storage (NEES), an Energy Frontier Research Center funded by the U.S. Department of Energy, Office of Science, Office of Basic Energy Sciences under Award Number DESC0001160. The authors acknowledge valuable discussions with Dr. Pradeep Ramiah Rajasekaran.

**Supporting Information Available:** Cyclic voltammogram of gold nanotube membrane in degassed 0.01 M KCl. This material is available free of charge *via* the Internet at <http://pubs.acs.org>.

## REFERENCES AND NOTES

1. Peighambari, S. J.; Rowshanzamir, S.; Amjadi, M. Review of the Proton Exchange Membranes for Fuel Cell Applications. *Int. J. Hydrogen Energy* **2010**, *35*, 9349–9384.
2. Xu, T. W. Ion Exchange Membranes: State of Their Development and Perspective. *J. Membr. Sci.* **2005**, *263*, 1–29.
3. Leung, P. K.; Xu, Q.; Zhao, T. S.; Zeng, L.; Zhang, C. Preparation of Silica Nanocomposite Anion-Exchange

- Membranes with Low Vanadium-Ion Crossover for Vanadium Redox Flow Batteries. *Electrochim. Acta* **2013**, *105*, 584–592.
- Arora, P.; Zhang, Z. M. Battery Separators. *Chem. Rev.* **2004**, *104*, 4419–4462.
  - Zhang, S. S. A Review on the Separators of Liquid Electrolyte Li-Ion Batteries. *J. Power Sources* **2007**, *164*, 351–364.
  - Elvington, M. C.; Colon-Mercado, H.; McCatty, S.; Stone, S. G.; Hobbs, D. T. Evaluation of Proton-Conducting Membranes for Use in a Sulfur Dioxide Depolarized Electrolyzer. *J. Power Sources* **2010**, *195*, 2823–2829.
  - Siwy, Z.; Heins, E.; Harrell, C. C.; Kohli, P.; Martin, C. R. Conical-Nanotube Ion-Current Rectifiers: The Role of Surface Charge. *J. Am. Chem. Soc.* **2004**, *126*, 10850–10851.
  - Kang, M. S.; Martin, C. R. Investigations of Potential-Dependent Fluxes of Ionic Permeates in Gold Nanotubule Membranes Prepared via the Template Method. *Langmuir* **2001**, *17*, 2753–2759.
  - Nishizawa, M.; Menon, V. P.; Martin, C. R. Metal Nanotubule Membranes with Electrochemically Switchable Ion-Transport Selectivity. *Science* **1995**, *268*, 700–702.
  - Lee, S. B.; Martin, C. R. Electromodulated Molecular Transport in Gold-Nanotube Membranes. *J. Am. Chem. Soc.* **2002**, *124*, 11850–11851.
  - Martin, C. R.; Nishizawa, M.; Jirage, K.; Kang, M. S.; Lee, S. B. Controlling Ion-Transport Selectivity in Gold Nanotubule Membranes. *Adv. Mater.* **2001**, *13*, 1351–1362.
  - Martin, C. R.; Nishizawa, M.; Jirage, K.; Kang, M. Investigations of the Transport Properties of Gold Nanotubule Membranes. *J. Phys. Chem. B* **2001**, *105*, 1925–1934.
  - Buyukserin, F.; Kohli, P.; Wirtz, M. O.; Martin, C. R. Electroactive Nanotube Membranes and Redox-Gating. *Small* **2007**, *3*, 266–270.
  - Martin, C. R. Nanomaterials: A Membrane-Based Synthetic Approach. *Science* **1994**, *266*, 1961–1966.
  - Martin, C. R. Membrane-Based Synthesis of Nanomaterials. *Chem. Mater.* **1996**, *8*, 1739–1746.
  - Wang, Q.; Cha, C. S.; Lu, J. T.; Zhuang, L. Ionic Conductivity of Pure Water in Charged Porous Matrix. *ChemPhysChem* **2012**, *13*, 514–519.
  - Bard, A. J.; Faulkner, L. R. *Electrochemical Methods: Fundamentals and Applications*, 2nd ed.; Wiley: New York, 2001; p 11.
  - Fosdick, S. E.; Knust, K. N.; Scida, K.; Crooks, R. M. Bipolar Electrochemistry. *Angew. Chem., Int. Ed.* **2013**, *52*, 10438–10456.
  - Harrell, C. C.; Lee, S. B.; Martin, C. R. Synthetic Single-Nanopore and Nanotube Membranes. *Anal. Chem.* **2003**, *75*, 6861–6867.
  - Bard, A. J.; Faulkner, L. R. *Electrochemical Methods: Fundamentals and Applications*, 2nd ed.; Wiley: New York, 2001; pp 547–549.
  - Bard, A. J.; Faulkner, L. R. *Electrochemical Methods: Fundamentals and Applications*, 2nd ed.; Wiley: New York, 2001; p 540.
  - Clavilli, J.; Vanhuong, N. Influence of Electrolyte Concentration on Differential-Potential Capacity Curves of a Gold Electrode in Contact with Aqueous Potassium Nitrate Solutions. *C. R. Acad. Sci., Ser. C* **1968**, *267*, 207–210.
  - Bard, A. J.; Faulkner, L. R. *Electrochemical Methods: Fundamentals and Applications*, 2nd ed.; Wiley: New York, 2001; p 68.
  - Kolics, A. R.; Thomas, A. E.; Wieckowski, A.  $^{36}\text{Cl}$  Labelling and Electrochemical Study of Chloride Adsorption on a Gold Electrode from Perchloric Acid Media. *J. Chem. Soc., Faraday Trans.* **1996**, *92*, 3727–3736.
  - Shi, Z. C.; Lipkowski, J. Chloride Adsorption at the Au(111) Electrode Surface. *J. Electroanal. Chem.* **1996**, *403*, 225–239.
  - Baker, T. A.; Friend, C. M.; Kaxiras, E. J. Nature of Cl Bonding on the Au (111) Surface: Evidence of a Mainly Covalent Interaction. *J. Am. Chem. Soc.* **2008**, *130*, 3720–3721.
  - Magnussen, O. M.; Ocko, B. M.; Adzic, R. R.; Wang, J. X. X-ray Diffraction Studies of Ordered Chloride and Bromide Monolayers at the Au(111)–Solution Interface. *Phys. Rev. B* **1995**, *51*, 5510–5513.
  - Luo, Y. R. *Comprehensive Handbook of Chemical Bond Energies*; CRC Press: Boca Raton, FL, 2007; p 1013.
  - Shi, Z. C.; Wu, S. J.; Lipkowski, J. Coadsorption of Metal Atoms and Anions: Cu UPD in the Presence of  $\text{SO}_4^{2-}$ ,  $\text{Cl}^-$ , and  $\text{Br}^-$ . *Electrochim. Acta* **1995**, *40*, 9–15.
  - Xu, K. Nonaqueous Liquid Electrolytes for Lithium-Based Rechargeable Batteries. *Chem. Rev.* **2004**, *104*, 4303–4417.
  - Menon, V. P.; Martin, C. R. Fabrication and Evaluation of Nanoelectrode Ensembles. *Anal. Chem.* **1995**, *67*, 1920–1928.
  - Kohli, P.; Wharton, J. E.; Braide, O.; Martin, C. R. Template Synthesis of Gold Nanotubes in an Anodic Alumina Membrane. *J. Nanosci. Nanotechnol.* **2004**, *4*, 605–610.
  - Miller, S. A.; Martin, C. R. Redox Modulation of Electroosmotic Flow in a Carbon Nanotube Membrane. *J. Am. Chem. Soc.* **2004**, *126*, 6226–6227.
  - Che, G. L.; Miller, S. A.; Fisher, E. R.; Martin, C. R. An Electrochemically Driven Actuator Based on a Nanostructured Carbon Material. *Anal. Chem.* **1999**, *71*, 3187–3191.
  - Che, G. L.; Lakshmi, B. B.; Fisher, E. R.; Martin, C. R. Carbon Nanotubule Membranes for Electrochemical Energy Storage and Production. *Nature* **1998**, *393*, 346–349.
  - Lee, S. B.; Martin, C. R. Controlling the Transport Properties of Gold Nanotubule Membranes Using Chemisorbed Thiols. *Chem. Mater.* **2001**, *13*, 3236–3244.
  - Kalman, E. B.; Sudre, O.; Vlassioug, I.; Siwy, Z. S. Control of Ionic Transport through Gated Single Conical Nanopores. *Anal. Bioanal. Chem.* **2009**, *394*, 413–419.
  - Heins, E. A.; Baker, L. A.; Siwy, Z. S.; Mota, M.; Martin, C. R. Effect of Crown Ether on Ion Currents through Synthetic Membranes Containing a Single Conically Shaped Nanopore. *J. Phys. Chem. B* **2005**, *109*, 18400–18407.